An Effective CTL Peptide Vaccine for Ebola Zaire Based on Survivors' CD8+ Targeting of a Particular Nucleocapsid Protein Epitope with Potential Implications for COVID-19 Vaccine Design SUPPLEMENTARY MATERIAL

1. Mitigating Potential for Epitope Competitive Inhibition at the MHC

The possibility of competitive inhibition at the MHC when a CTL vaccine containing multiple peptides is administered to a patient has been acknowledged [4]. Techniques such as splitting a CTL vaccine dose across multiple injection sites with one peptide sequence per site have been suggested to address this issue [8]. We demonstrated *in-vitro* that competitive inhibition at the MHC could occur by incubating 200,000 PBMCs per well from a reference PMBC sample (CTL Reference Sample QC Set, Cellular Technology, Ltd. Shaker Heights, Ohio), from an HLA A*02, HIV naive subject with an HCMV Class I epitope pp65 (495-503) NLVPMVATV supplied with the Reference Sample and known to produce $IFN-\gamma$ release in that reference PBMC sample and then introducing increasing concentrations of of an HLA A*02 matched Class I HIV peptide. Figure 9 shows functional inhibition of MHC binding as evidenced by decreasing, and ultimate extinction of $IFN-\gamma$ release as determined by ELISA assay with increasing concentrations of the HLA matched HIV peptide. This experiment suggests that competitive inhibition could occur when two different HLA matched peptide sequences are delivered to the same antigen presenting cell. The adjuvanted microspheres used in this study were manufactured to be nominally the same same size as antigen presenting cells (about 11μM). By loading each peptide microsphere with only one peptide sequence, this mitigates

against two peptides being processed by the same antigen presenting cell at the same time. Multiple peptides can be incorporated into a vaccine formulation by blending different populations of adjuvanted microspheres into the same vaccine dose, with each microsphere containing only one peptide sequence.

2. Route of Administration

Intradermal injection of influenza vaccine has been shown to be more effective than intramuscular administration in human subjects [3]. Gamma scintigraphy studies have shown that the efficacy of intradermally-delivered antigen may be due to the portion of antigen that reaches the lymph system [9]. The rat peritoneal space has been demonstrated to drain into the rat lymphatics [5]. We sought to determine if H2D-Kb matched Class I epitopes delivered into the mouse intraperitoneal space with Class II eptiopes would provide a stronger immune response by ELISPOT-determined $IFN-\gamma$ release compared with intradermal and intramuscular administration to C57BL/6 mice.

Prior to conducting our challenge study, we used adjuvanted microspheres to immunize C57BL/6 mice [6]. OVA and VSV Class I and Class II epitopes known to produce an immune response in this mouse model were selected and delivered by three different routes of administration [2] [10] [7] [1]. Four different microsphere populations, each containing CpG and one of the epitopes from Table 14, were prepared. The four microsphere populations were blended 1:1:1:1 by weight and suspended just prior to administration in a PBS injectate solution containing MPLA. A total of 2mg of the microsphere preparation was administered into C57BL/6 mice by the intradermal tail (ID), intramuscular (IM) or intraperitoneal (IP) route using four mice for each route of administration. Splenocytes were harvested on day 14 and subjected to ELISPOT analysis evaluating $IFN-\gamma$ release in response to stimulation with the peptide used in the vaccination. As illustrated in Figure 11 and Figure 10, the CTL response to each of the administered Class I epitopes was significantly higher for the IP route of administration. Guided by this data, we selected IP as the route of

vaccine administration for our EBOV challenge study.

3. Vaccine Formulation Composition

Adjuvanted microspheres nominally 11μM in diameter (geometric standard deviation 1.2) manufactured as a room temperature stable dry powder and loaded as described in Table 12 are mixed with the injectate solution described in Table 13 just prior to injection. All mice in the EBOV challenge study received nominally 450μl of this adjuvanted microsphere suspension by intraperitoneal administration.

4. Separation of CD4 & CD8 T-cells for ELISPOT

Mouse spleens were harvested and splenocytes were obtained by standard procedures. Splenocytes were counted and divided into three equal groups; one for total cell response in the ELISPOT assay, one for the ELISPOT response in the absence of CD4 cells, and the final group for the ELISPOT response in the absence of CD8 cells. CD4 and CD8 cells were removed by positive selection using magnetic beads coated with either anti-CD4 or anti-CD8 antibody respectively, and a MACS Separator (Miltenyi Biotech, Auburn, CA) according to the manufacturer's instructions. Cells not bound to the columns (i.e., unlabeled by the specific antibody) were collected, centrifuged, washed, re-centrifuged, counted, and placed in a standard ELISPOT assay as previously described.

Mouse Observation Clinical Scores

Scale	Description of Animal
1	Healthy
2	Lethargic and/or ruffled fur (triggers a second observation)
3	Ruffled fur, lethargic and hunched posture, orbital tightening (triggers a third observation)
4	Ruffled fur, lethargic, hunched posture, orbital tightening reluctance to move when stimulated, paralysis or greater than 20% weight loss (requires immediate euthanasia)

Table 1: Clinical score indices used to track morbidity in study animals.

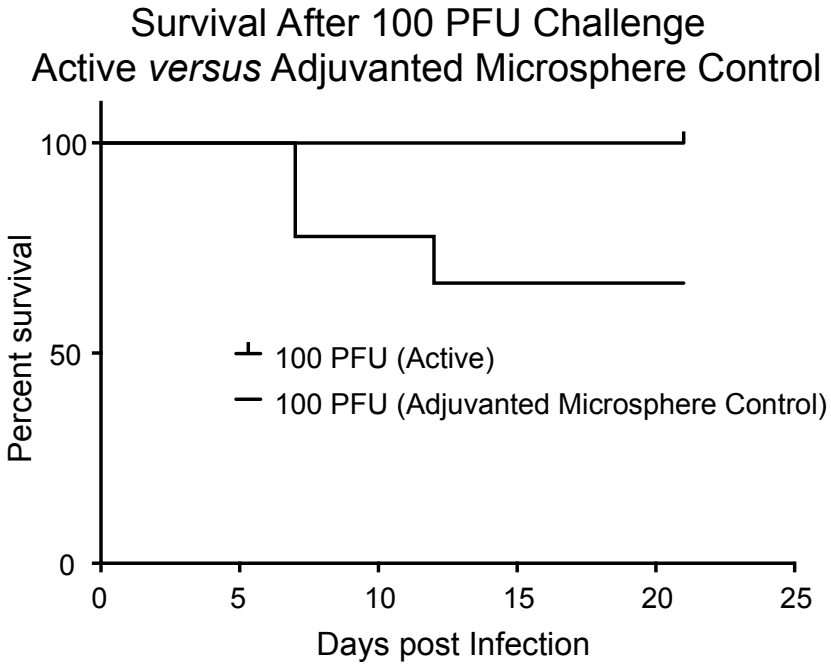

(a) Survival curve *versus* Adjuvanted Microsphere Control.

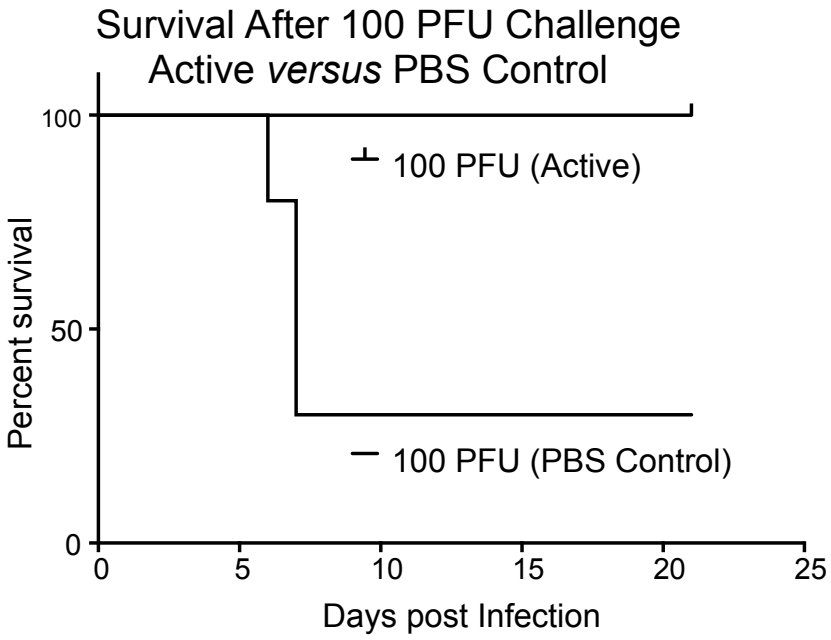

(b) Survival curve *versus* PBS buffer control.

Figure 1: The 100PFU PBS control survival curve 1b is not statistically different from the 100PFU adjuvanted control survival curve 1a. A chi square test results in a P = 0.37 for (survived / dead) 6/4 (adjuvanted) versus 3/7 (PBS control).

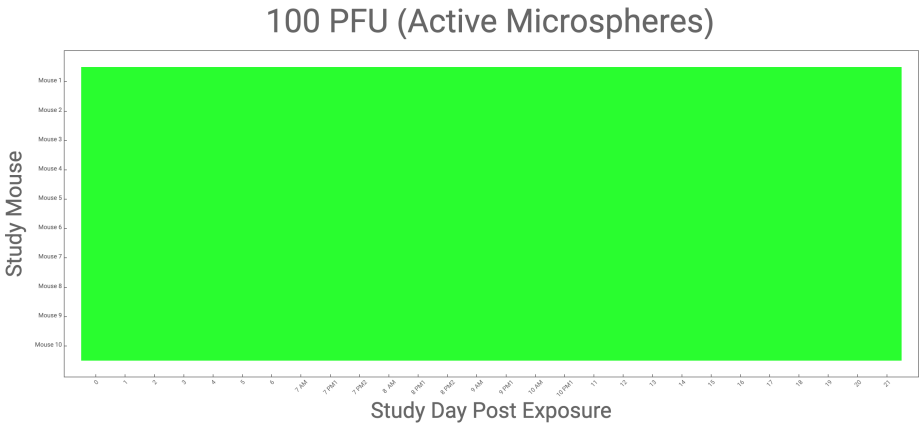

Figure 2: Clinical observations showing that no mice died in this group during the study, scored from 1 (healthy) to 4 (moribund) made post infection in control animals receiving PBS buffer via intraperitoneal injection 14 days before infection. The clinical scores described in Table 1 are shown using the following color scheme: 1 = GREEN, 2 = YELLOW, 3 = ORANGE and 4 = RED. A dead mouse is coded in black. The frequency of measurements was increased on post infection days 6-9 coinciding with the anticipated period of peak morbidity.

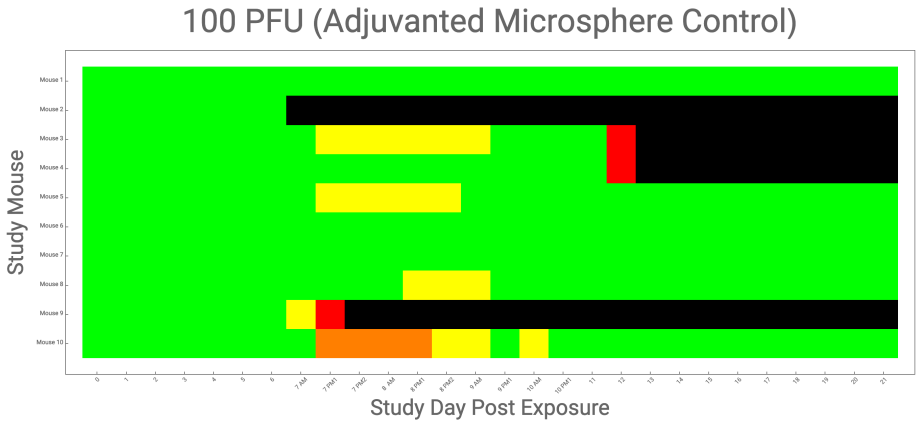

Figure 3: Clinical observations, scored from 1 (healthy) to 4 (moribund) made post infection in control animals receiving PBS buffer via intraperitoneal injection 14 days before infection. The clinical scores described in Table 1 are shown using the following color scheme: 1 = GREEN, 2 = YELLOW, 3 = ORANGE and 4 = RED. A dead mouse is coded in black. The frequency of measurements was increased on post infection days 6-9 coinciding with the anticipated period of peak morbidity.

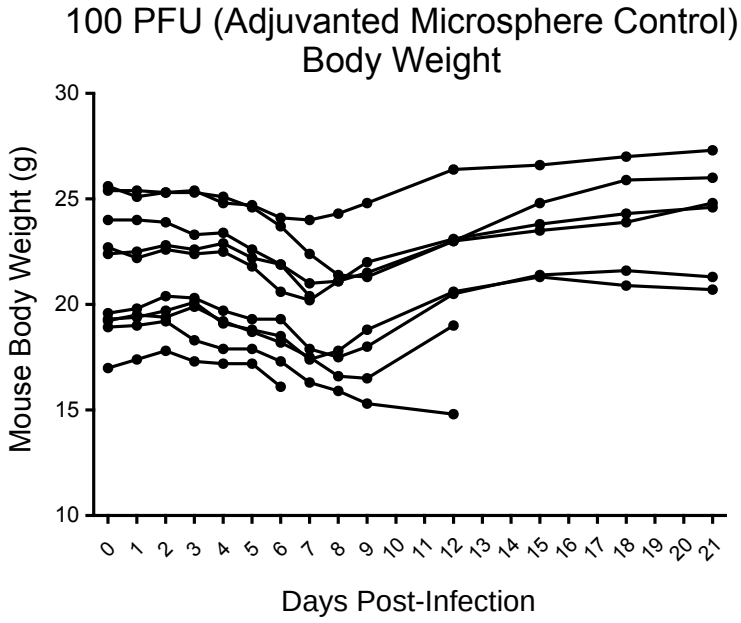

Figure 4: Daily weights were recorded post infection. Measurements for control animals, receiving adjuvanted microspheres 14 days before infection, are shown here.

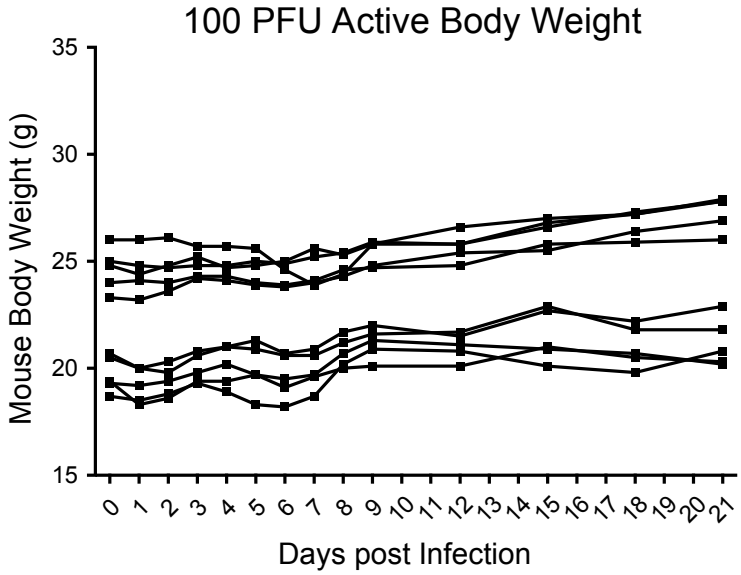

Figure 5: Daily weights were recorded post infection. Measurements for animals receiving active vaccine 14 days before infection, are shown here.

Figure 6: NP44-52 has conserved residues across three strains of EBOV.

Computed HLA Binding Affinities for YQVNNLEEI

Allele	Median $pIC_{50}nM$	Consensus Score
HLA-A*02:06	5.8	0.16
HLA-A*02:03	106	2.4
HLA-A*02:01	198	3.7
HLA-B*15:01	791	4.7
HLA-A*23:01	1140	2.1
HLA-B*40:01	1140	2.4
HLA-A*68:02	5553	23
HLA-A*24:02	5664	5.7
HLA-B*53:01	8737	15
HLA-B*58:01	12128	17
HLA-B*51:01	13551	6.3
HLA-A*26:01	15442	11
HLA-A*32:01	17173	22
HLA-B*44:03	18798	17
HLA-B*35:01	19374	35
HLA-A*30:01	23549	61
HLA-B*44:02	27488	20
HLA-A*30:02	31424	55

Table 2: Database-predicted HLA binding affinities for NP44-52 (YQVNNLEEI), the Class I peptide used in this study.

Computed H-2 Binding Affinities for YQVNNLEEI

Allele	Median $pIC_{50}nM$	Consensus Score
H-2-D^{b}	26	0.20
H-2-K^{d}	5639	7.0
H-2-K^{b}	13722	32
H-2-D^{d}	21052	23
H-2-L^{d}	-	41

Table 3: Database-predicted H-2 binding affinities for NP44-52 (YQVNNLEEI), the Class I peptide used in this study.

Computed HLA-DR Binding Affinities for VKNEVNSFKAALSSLAKHG

Allele	Start	15-mer peptide	Median pIC_{50}nM	Consensus Score
HLA-DRB1*01:01	5	VNSFKAALSSLAKHG	4.1	0.28
HLA-DRB1*09:01	5	VNSFKAALSSLAKHG	6.0	0.010
HLA-DRB1*04:05	4	EVNSFKAALSSLAKH	14	0.19
HLA-DRB5*01:01	5	VNSFKAALSSLAKHG	24	1.8
HLA-DQA1*05:01/DQB1*03:01	3	NEVNSFKAALSSLAK	24	13
HLA-DRB1*04:01	5	VNSFKAALSSLAKHG	25	1.2
HLA-DPA1*02:01/DPB1*14:01	4	EVNSFKAALSSLAKH	27	4.7
HLA-DRB3*02:02	4	EVNSFKAALSSLAKH	27	0.080
HLA-DRB1*07:01	2	KNEVNSFKAALSSLA	40	4.7
HLA-DRB1*11:01	5	VNSFKAALSSLAKHG	66	4.3
HLA-DRB1*15:01	3	NEVNSFKAALSSLAK	152	3.4
HLA-DRB1*08:02	3	NEVNSFKAALSSLAK	162	1.4
HLA-DQA1*01:02/DQB1*06:02	3	NEVNSFKAALSSLAK	167	6.2
HLA-DPA1*02:01/DPB1*01:01	4	EVNSFKAALSSLAKH	401	26
HLA-DRB1*12:01	5	VNSFKAALSSLAKHG	769	8.8
HLA-DPA1*03:01/DPB1*04:02	4	EVNSFKAALSSLAKH	773	15
HLA-DRB4*01:01	3	NEVNSFKAALSSLAK	903	37
HLA-DRB1*13:02	1	VKNEVNSFKAALSSL	1380	28
HLA-DRB1*03:01	2	KNEVNSFKAALSSLA	1498	13
HLA-DQA1*03:01/DQB1*03:02	1	VKNEVNSFKAALSSL	1680	21
HLA-DPA1*02:01/DPB1*05:01	5	VNSFKAALSSLAKHG	1811	25
HLA-DQA1*04:01/DQB1*04:02	4	EVNSFKAALSSLAKH	1951	16
HLA-DRB3*01:01	2	KNEVNSFKAALSSLA	1991	21
HLA-DPA1*01:03/DPB1*02:01	4	EVNSFKAALSSLAKH	2002	26
HLA-DPA1*01/DPB1*04:01	4	EVNSFKAALSSLAKH	2073	31
HLA-DQA1*05:01/DQB1*02:01	2	KNEVNSFKAALSSLA	3341	32
HLA-DQA1*01:01/DQB1*05:01	1	VKNEVNSFKAALSSL	3922	29

Table 4: Database-predicted HLA binding affinities for VKNEVNSFKAALSSLAKHG, the Class II peptide used in this study.

Computed H2-I Binding Affinities for
VKNEVNSFKAALSSLAKHG

Allele	Start	15-mer peptide	Median $pIC_{50}nM$	Consensus Score
H2-IA^{b}	4	EVNSFKAALSSLAKH	138	1.4
H2-IA^{d}	5	VNSFKAALSSLAKHG	1069	6.1
H2-IE^{d}	5	VNSFKAALSSLAKHG	5797	35

Table 5: Database-predicted H2-I binding affinities for VKNEVNSFKAALSSLAKHG, the Class II peptide used in this study.

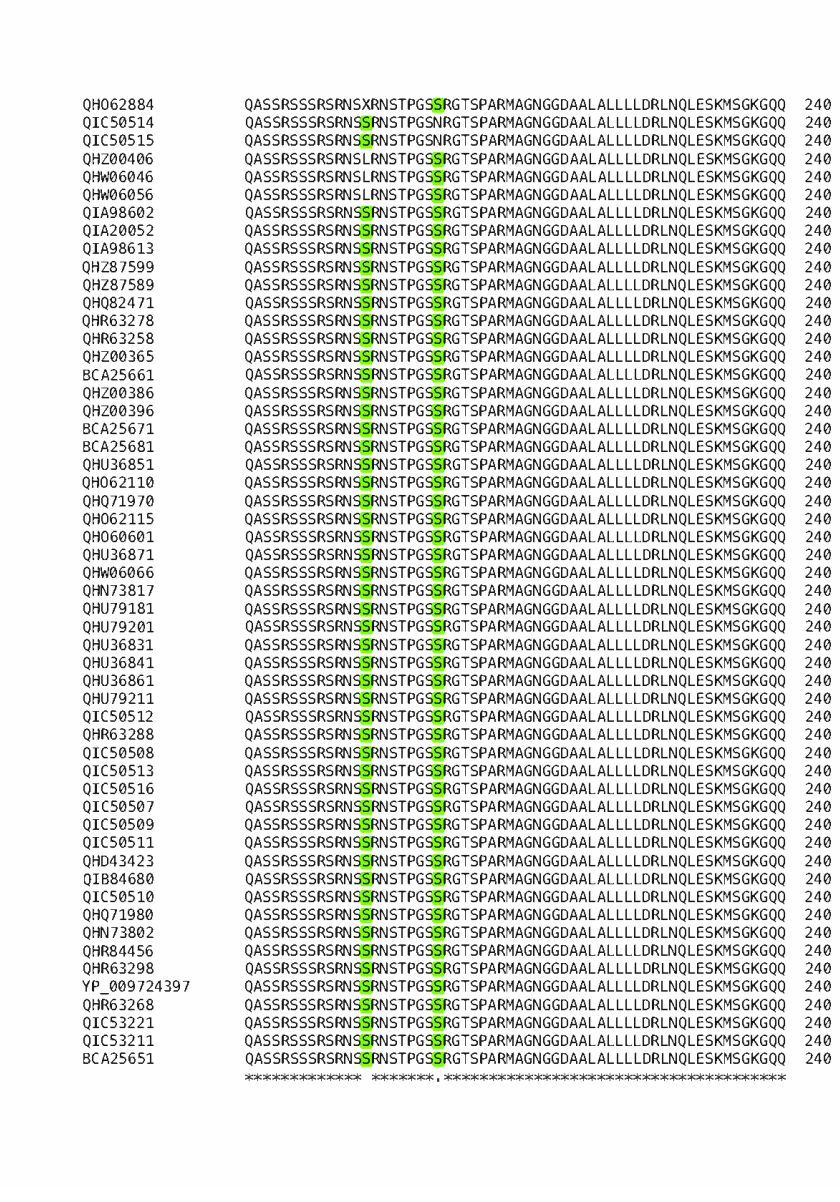

Figure 7: Part 1 of 2. Sequences from 54 subjects with COVID-19 were found to have highly conserved nucleocapsid peptide sequences from positions 1-419 with the exception of three positions. At position 194, three individual sequences differ with non-conserved amino acid residues and one unknown amino acid. At position 202, a partially conserved amino acid variant is seen in two samples. At position 344, one non-conserved amino acid is present, however, this sample used a laboratory host cell line where only one of 4 replicates displayed this non-conserved amino acid substitution. These three mutation positions are colored according to the Clustal X color scheme.

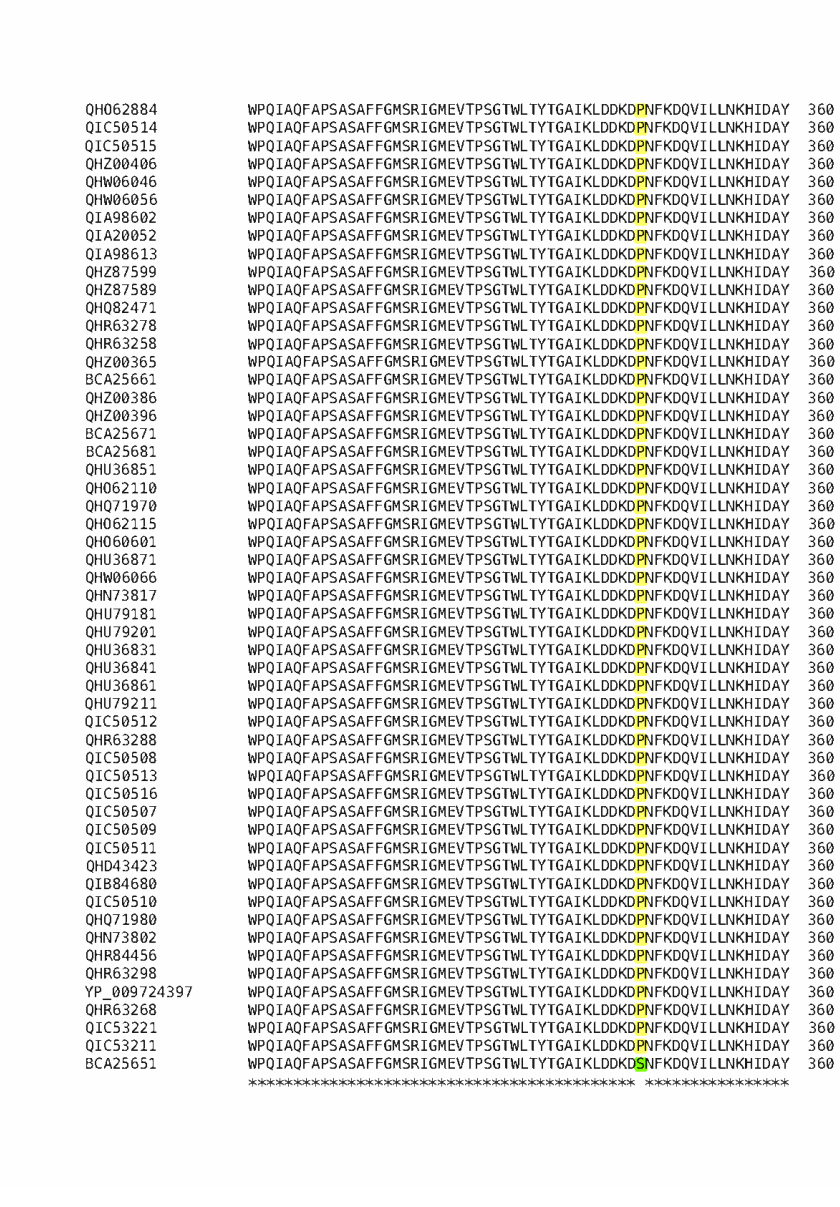

Figure 8: Part 2 of 2. Sequences from 54 subjects with COVID-19 were found to have highly conserved nucleocapsid peptide sequences from positions 1-419 with the exception of three positions. At position 194, three individual sequences differ with non-conserved amino acid residues and one unknown amino acid. At position 202, a partially conserved amino acid variant is seen in two samples. At position 344, one non-conserved amino acid is present, however, this sample used a laboratory host cell line where only one of 4 replicates displayed this non-conserved amino acid substitution. These three mutation positions are colored according to the Clustal X color scheme.

COVID-19 Nucleocapsid Peptides with Associated Predicted HLA Restricted Binding Affinities (1/4)

Peptide	Start Position	Allele	NetMHC 4.0 pIC_{50}nM	NetMHCpan 4.0 pIC_{50}nM	SARS Same?
LSPRWYFYY	104	HLA-A*01:01	48.64	76.9	YES
LLLDRLNQL	222	HLA-A*02:01	14.81	11.3	YES
GMSRIGMEV	316	HLA-A*02:01	50.61	48.1	YES
KTFPPTEPK	361	HLA-A*03:01	20.8	18.8	YES
KSAAEASKK	249	HLA-A*03:01	116.22	139.4	YES
LIRQGTDYK	291	HLA-A*03:01	274.69	137.5	YES
ASAFFGMSR	311	HLA-A*03:01	292.41	285.3	YES
QLESKMSGK	229	HLA-A*03:01	322.41	751	NO
FTALTQHGK	53	HLA-A*03:01	788.84	345.5	YES
KTFPPTEPK	361	HLA-A*11:01	6.28	7.7	YES
ASAFFGMSR	311	HLA-A*11:01	14.4	15.3	YES
FTALTQHGK	53	HLA-A*11:01	127.28	44.9	YES
KSAAEASKK	249	HLA-A*11:01	76.73	62.2	YES
AGLPYGANK	119	HLA-A*11:01	240.23	157.5	NO
LIRQGTDYK	291	HLA-A*11:01	984.82	160.6	YES
LSPRWYFYY	104	HLA-A*11:01	253.34	492.8	YES
TQALPQRQK	379	HLA-A*11:01	740.66	415.1	NO
QQQGQTVTK	240	HLA-A*11:01	428.26	470.3	YES
KHIDAYKTF	355	HLA-A*23:01	134.12	778.7	YES
YYRRATRRI	86	HLA-A*23:01	151.38	366.6	NO
TWLTYTGAI	329	HLA-A*23:01	24164.38	282.1	NO
KHWPQIAQF	299	HLA-A*23:01	317.71	313.7	YES
KAYNVTQAF	266	HLA-A*23:01	341.14	602.3	NO
YYRRATRRI	86	HLA-A*24:02	74.89	322	NO

Table 6: This set of 53 unique peptides (part 1 of 4) achieves > 95% world-wide population coverage. The starting position is within the nucleocapsid. Peptides chosen with binding affinity predictions less than 500nm via NetMHC 4.0 or NetMHCpan 4.0. Peptide sequences colored in red have literature references as known *in-vitro* binders to the predicted allele match (see text).

COVID-19 Nucleocapsid Peptides with Associated Predicted HLA Restricted Binding Affinities (2/4)

Peptide	Start Position	Allele	NetMHC 4.0 $pIC_{50}nM$	NetMHCpan 4.0 $pIC_{50}nM$	SARS Same?
FAPSASAFF	307	HLA-A*24:02	422.31	847.7	YES
NTASWFTAL	48	HLA-A*26:01	1113.04	122.6	YES
ELIRQGTDY	290	HLA-A*26:01	652.8	327.8	NO
FAPSASAFF	307	HLA-A*26:01	349.57	606.6	YES
IGYYRRATR	84	HLA-A*33:03	N/A	57.8	YES
NVTQAFGRR	269	HLA-A*33:03	N/A	62.5	YES
ASAFFGMSR	311	HLA-A*33:03	N/A	149.3	YES
QASSRSSSR	181	HLA-A*33:03	N/A	163.9	YES
YNVTQAFGR	268	HLA-A*33:03	N/A	189.1	YES
GYYRRATRR	85	HLA-A*33:03	N/A	359.4	YES
SSRSSSRSR	183	HLA-A*33:03	N/A	395.3	YES
FPRGQGVPI	66	HLA-B*07:02	3.82	4.7	YES
KPRQKRTAT	257	HLA-B*07:02	4.42	18.8	YES
SPRWYFYYL	105	HLA-B*07:02	6.32	15.3	YES
RIRGGDGKM	93	HLA-B*07:02	149.86	173	NO
NPANNAAIV	150	HLA-B*07:02	184.8	569.3	NO
LPNNTASWF	45	HLA-B*07:02	244.3	334	YES
SPRWYFYYL	105	HLA-B*08:01	13.77	42.1	YES
LLLDRLNQL	222	HLA-B*08:01	125.72	136.8	YES
FPRGQGVPI	66	HLA-B*08:01	245.35	368.3	YES
KPRQKRTAT	257	HLA-B*08:01	364.72	432.6	YES
KAYNVTQAF	266	HLA-B*15:01	40.35	19	NO
LLNKHIDAY	352	HLA-B*15:01	33.04	32.5	YES

Table 7: This set of 53 unique peptides (part 2 of 4) achieves > 95% world-wide population coverage. The starting position is within the nucleocapsid. Peptides chosen with binding affinity predictions less than 500nm via NetMHC 4.0 or NetMHCpan 4.0. Peptide sequences colored in red have literature references as known *in-vitro* binders to the predicted allele match (see text).

COVID-19 Nucleocapsid Peptides with Associated Predicted HLA Restricted Binding Affinities (3/4)

Peptide	Start Position	Allele	NetMHC 4.0 pIC_{50}nM	NetMHCpan 4.0 pIC_{50}nM	SARS Same?
LQLPQGTTL	159	HLA-B*15:01	105.55	229.8	YES
FAPSASAFF	307	HLA-B*15:01	213.11	281.9	YES
FSKQLQQSM	403	HLA-B*15:01	219.07	286	NO
RLNQLESKM	226	HLA-B*15:01	1496.11	490.3	NO
QFAPSASAF	306	HLA-B*15:01	493.85	700.3	YES
RRIRGGDGK	92	HLA-B*27:05	65.94	72.5	NO
RRATRRIRG	88	HLA-B*27:05	253.64	787.8	NO
QRNAPRITF	9	HLA-B*27:05	560.56	262.1	NO
YRRATRRIR	87	HLA-B*27:05	415.31	597.7	NO
NTASWFTAL	48	HLA-B*39:01	47.87	353.3	YES
KKADETQAL	374	HLA-B*39:01	137.43	926.4	NO
LQLPQGTTL	159	HLA-B*39:01	238.19	228.7	YES
TRNPANNAA	148	HLA-B*39:01	406.62	818.3	NO
MEVTPSGTW	322	HLA-B*44:02	11.48	14.2	YES
LPNNTASWF	45	HLA-B*53:01	19.03	25.7	YES
TPSGTWLTY	325	HLA-B*53:01	26.99	79	YES
LPAADLDDF	395	HLA-B*53:01	193.75	74.8	NO
FAPSASAFF	307	HLA-B*53:01	1164.6	317.4	YES
GANKDGIIW	124	HLA-B*53:01	320.56	1015.8	NO
KAYNVTQAF	266	HLA-B*58:01	12.51	17.7	NO
GANKDGIIW	124	HLA-B*58:01	158.07	35.3	NO
KMKDLSPRW	100	HLA-B*58:01	83.99	99.2	NO
LSPRWYFYY	104	HLA-B*58:01	359.42	430.6	YES
KAYNVTQAF	266	HLA-C*03:04	N/A	12.7	NO

Table 8: This set of 53 unique peptides (part 3 of 4) achieves > 95% world-wide population coverage. The starting position is within the nucleocapsid. Peptides chosen with binding affinity predictions less than 500nm via NetMHC 4.0 or NetMHCpan 4.0. Peptide sequences colored in red have literature references as known *in-vitro* binders to the predicted allele match (see text).

COVID-19 nucleocapsid Peptides with Associated Predicted HLA Restricted Binding Affinities (4/4)

Peptide	Start Position	Allele	NetMHC 4.0 pIC_{50}nM	NetMHCpan 4.0 pIC_{50}nM	SARS Same?
FAPSASAFF	307	HLA-C*03:04	N/A	41.4	YES
LTYTGAIKL	331	HLA-C*03:04	N/A	44.8	NO
NTASWFTAL	48	HLA-C*03:04	N/A	58.8	YES
SAFFGMSRI	312	HLA-C*03:04	N/A	68	YES
LQLPQGTTL	159	HLA-C*03:04	N/A	99.5	YES
FSKQLQQSM	403	HLA-C*03:04	N/A	149.9	NO
FPRGQGVPI	66	HLA-C*03:04	N/A	434.9	YES
YRRATRRIR	87	HLA-C*07:01	112.27	8786.2	NO
QRNAPRITF	9	HLA-C*07:01	1337.36	198.9	NO
YYRRATRRI	86	HLA-C*07:01	254.32	957.2	NO
LKFPRGQGV	64	HLA-C*07:01	446.18	1633.3	NO
QRNAPRITF	9	HLA-C*07:02	261.17	237.8	NO
YYRRATRRI	86	HLA-C*07:02	6229.2	242.2	NO
FAPSASAFF	307	HLA-C*07:02	16893.5	347.4	YES
KHWPQIAQF	299	HLA-C*07:02	430.68	971.3	YES
NFKDQVILL	345	HLA-C*07:02	29905.43	462.1	NO
KAYNVTQAF	266	HLA-C*07:02	668.01	477	NO
FAPSASAFF	307	HLA-C*08:01	N/A	280.1	YES
KAYNVTQAF	266	HLA-C*08:01	N/A	412.2	NO

Table 9: This set of 53 unique peptides (part 4 of 4) achieves > 95% world-wide population coverage. The starting position is within the nucleocapsid. Peptides chosen with binding affinity predictions less than 500nm via NetMHC 4.0 or NetMHCpan 4.0. Peptide sequences colored in red have literature references as known *in-vitro* binders to the predicted allele match (see text).

Projected World-Wide Population Coverage for a COVID-19 Peptide Vaccine Targeting 9mer Peptides on Nucleocapsid Proteins

Minimum Epitope Matches / Allele / Person	% Projected Coverage	Cumulative % Population Coverage
1	18.14	97.27
2	35.05	79.13
3	29.7	44.08
4	12.02	14.37
5	2.2	2.35
6	0.15	0.15

Table 10: Data showing projected HLA world-wide population coverage for a COVID-19 vaccine using the 16 epitopes listed in Tables 6 through 9. If we assume a least one HLA match per peptide capable of producing a clinically relevant immune response in a person, we can achieve 97.27% global population coverage with a 16 Class I peptide CTL vaccine.

Projected China-Specific Population Coverage for a COVID-19 Peptide Vaccine Targeting 9mer Peptides on Nucleocapsid Proteins

Minimum Epitope Matches / Allele / Person	% Projected Coverage	Cumulative % Population Coverage
1	26.02	94.39
2	38.01	68.37
3	23.14	30.36
4	6.42	7.22
5	0.77	0.8
6	0.03	0.03

Table 11: If we take the assumptions made in the global projected population coverage Table 10 now assuming a China-specific HLA distribution, we still can achieve 94.39% population coverage

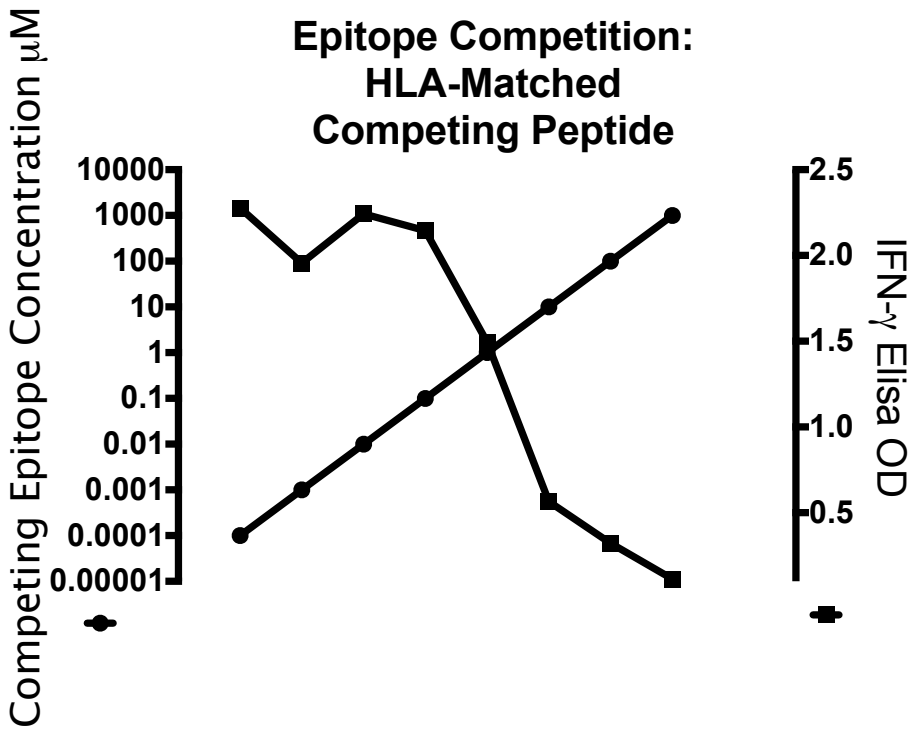

Figure 9: Simultaneous *in-vitro* incubation of two HLA matched epitopes to human PBMCs from an indivdual vaccinated against tetanus toxin. $IFN-\gamma$ release in response to a Class I epitope from tetanus virus is inhibited by increasing concentrations of Class I epitope from HIV in a patient not exposed to the HIV virus.

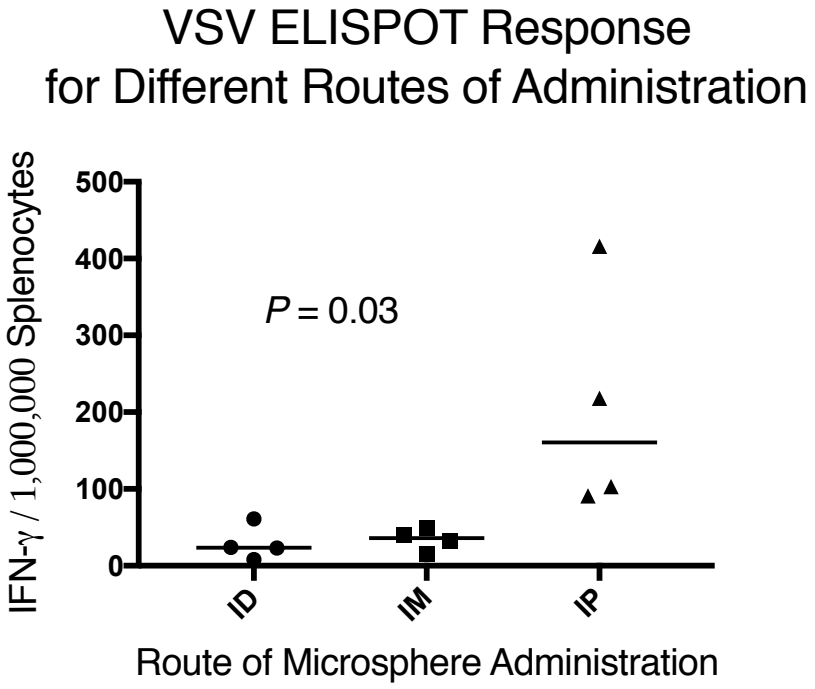

Figure 10: Differential ELISPOT response to intradermal tail (ID) intramuscular (IM) and intraperitoneal administration of 2mg of adjuvanted microspheres loaded with VSV Class I epitope RGYVYQGL.

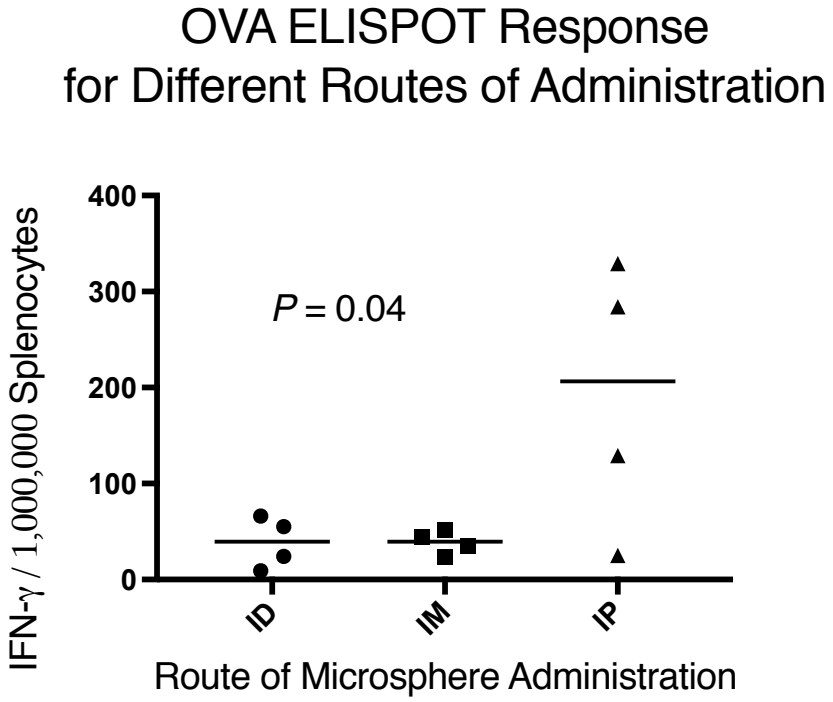

Figure 11: Differential ELISPOT response to intradermal tail (ID) intramuscular (IM) and intraperitoneal administration of 2mg of adjuvanted microspheres loaded with OVA Class I epitope RGYVYQGL.

Adjuvanted Microsphere Loaded Component	Amount
Peptide	0.1% w/w
CpG	0.025% w/w
Mannose	0.01% w/w

Table 12: Compositon of 11μM PLGA (Resomer 502H) adjuvanted microspheres used for the study.

Injectate Component	Amount
Polysorbate 20	0.01% (v/v)
MPLA	50μg/ml

Table 13: Compositon of PBS injectate used for the study.

Peptide Sequence	Description
SIINFEKL	OVA Class I
ISQAVHAAHAEINEAGR	OVA Class II
RGYVYQGL	VSV Class I
SSKAGVFEHPHIGDASSGL	VSV Class II

Table 14: Class I and Class II peptides used in the study. Any single microsphere used to inoculate mice for this study contained only one of the epitopes in this table.

References

[1] C Burkhart, G Freer, R Castro, L Adorini, KH Wiesmuller, RM Zinkernagel, and H Hengartner. Characterization of t-helper epitopes of the glycoprotein of vesicular stomatitis virus. *JOURNAL OF VIROLOGY*, pages 1573 – 1580, 1994. URL https://www.ncbi.nlm.nih.gov/pubmed/7508998.

[2] CM Celluzzi, JI Mayordomo, WJ Walter J. Storkus, MT Lotze, and LD Falo. Peptide-pulsed dendritic cells induce antigen-specific, ctl-mediated protective tumor immunity. *Journal of Exoperimental Medicine*, pages 283, 287, 1996. doi: DOI: 10.1084/jem.183.1.283.

[3] R Kenney, S Frech, L Muenz, C Villar, and G Glenn. Dose sparing with intradermal injection of influenza vaccine. *NEJM*, 351(6), 2004. doi: 10.1056/NEJMoa043540. URL https://doi.org/10.1056/NEJMoa043540.

[4] C Lock, D Smilek, A Gautam, M Vaysburd, S Dwivedy, and H McDevitt. Competitive inhibition of antigen presentation in animal models of autoimmune disease. In *Seminars in immunology*, volume 3, pages 247–255, 1991.

[5] CP Parungo, D Soybel, YL Colson, SW Kim, S Ohnishi, AM De Grand, RG Laurence, FY Chen, EG Soltesz, LH Cohn, MC Bawendi, and JV Frangioni. Lymphatic drainage of the peritoneal space: A pattern dependent on bowel lymphatics. *Ann Surg Oncol.*, 14(2):286–298, 2007. doi: DOI: 10.1245/s10434-006-9044-6.

[6] R. M. Rubsamen, C. V. Herst, P. M. Lloyd, and D. E. Heckerman. Eliciting cytotoxic t-lymphocyte responses from synthetic vectors containing one or two epitopes in a c57bl/6 mouse model using peptide-containing biodegradable microspheres and adjuvants. *Vaccine*, 32:4111–4116, 2014. doi: 10.1016/j.vaccine.2014.05.071. URL https://doi.org/10.1016/j.vaccine.2014.05.071.

[7] I Sakita, H Hörig, R Sun, F Wang, and SG Nathenson. In vivo ctl immunity can be elicited by in vitro reconstituted mhc/peptide complex. *Journal of Immunological Methods*, pages 105,115, 1996. doi: doi.org/10.1016/0022-1759(96)00027-0. URL https://doi.org/10.1016/0022-1759(96)00027-0.

[8] CL Slingluff. The present and future of peptide vaccines for cancer: Single or multiple, long or short, alone or in combination? *Cancer journal*, 17 (5):343–350, 2011. doi: 10.1097/PPO.0b013e318233e5b2. URL https://doi.org/10.1097/PPO.0b013e318233e5b2.

[9] M Tozuka, T Oka, N Jounal, G Egawa, and K Ishi. Efficient antigen delivery to the draining lymph nodes is a key component in the immunogenic pathway of the intradermal vaccine. *Dermatological Science*, 82 (8), 2015. doi: http://dx.doi.org/10.1016/j.jdermsci.2015.11.008. URL http://dx.doi.org/10.1016/j.jdermsci.2015.11.008.

[10] J Zhang, L De Masi, B John, W Chen, and DM Schifferli. In vivo ctl immunity can be elicited by in vitro reconstituted mhc/peptide complex. *icrobial Cell Factories*, 2014. doi: http://www.microbialcellfactories.com/content/13/1/80. URL http://www.microbialcellfactories.com/content/13/1/80.